

BaTiO₃ film grown by water-based process

Sarmad Fawzi Hamza Alhasan^{a,b}, Hussain Abouelkhair^c, Robert. E. Peale^c,
Isaiah. O. Oladeji^d

^a Department of Electrical and Computer Engineering, University of Central Florida,
Orlando, Florida 32816, USA

^b Laser and Optoelectronics Engineering Department, University of Technology,
Baghdad 10066, IRAQ

^c Department of Physics, University of Central Florida, Orlando, Florida 32816, USA

^d SISOM Thin Films LLC, Orlando, Florida 32805, USA

Self-assembled nano-crystalline BaTiO₃ films on stainless steel foil substrates, were grown by the water based **Streaming Process for Electrodeless Electrochemical Deposition (SPEED)**. SPEED is an aqueous process that deposits self-assembled nano-crystalline inorganic thin films over large areas, without a vacuum, providing a scalable and manufacturing friendly process to fabricate durable films. The morphology of the ~1 μm thick films comprises single crystals of micron dimensions imbedded in a matrix of nanocrystals. XRD confirms presence of BaTiO₃ crystals of hexagonal phase for samples annealed at 500 C. Subsequent annealing at 600 C transforms the film to the cubic phase. Potential applications include dielectric layers, capacitors, waveguides, ferroelectric RAM, pyroelectric infrared detectors, and phosphors. Characterization of infrared pyroelectric response at 10 μm wavelength shows an initially good sensitivity that reversibly decays over a period of days due to water vapor absorption. A short-lived photo-response due to poling of the hydrated sample is also observed.

Introduction

The inorganic compound barium titanate (BaTiO₃) is a member of the Perovskite family, which has the general formula ABO₃. BaTiO₃ has excellent dielectric, ferroelectric and piezoelectric properties. BaTiO₃ was the first ferroelectric ceramic, and it is a good candidate for a diverse applications due to its high permittivity and low loss (1). Applications include pyroelectric detectors (2), capacitors (3), waveguide modulators (4), gate dielectrics (5) and holographic memory (6).

The optimum synthesis method for BaTiO₃ depends on the end application, as the method used has a significant impact on the structure and properties of BaTiO₃. Its five known phases are hexagonal, cubic, tetragonal, orthorhombic, and rhombohedral. This paper considers the pyroelectric response to infrared radiation of BaTiO₃ thin films. Pyroelectric response is the appearance of a small voltage difference across opposite faces of the film due to a change in temperature that changes the film's intrinsic polarization. Of its 5 possible crystal classes, only the cubic phase is incapable by symmetry of being pyroelectric (7).

Methods of preparing BaTiO₃ include solid-state reaction (8), chemical methods (9), hydrothermal growth (10), sol-gel processing (11), spray pyrolysis (12), the oxalate route (13), microwave heating (14), a micro-emulsion process (15), a polymeric precursor method (16), nanometer oxides doping (17) and modified combustion process (18). We present a different method of thin film preparation, which is superficially similar to spray pyrolysis, except that it does not involve thermal splitting of molecules, and hence operates at lower temperature.

Experimental Details

Self-assembled nano-crystalline BaTiO₃ films on stainless steel foil substrates, were grown by the water-based Streaming Process for Electrodeless Electrochemical Deposition (SPEED), which deposits inorganic thin films over large areas, without a vacuum, a scalable and manufacturing friendly process. Water-soluble compounds with complexing agents grow films by heterogeneous reaction on the substrate, with little wasteful homogeneous reaction. Hydrophilic substrates bind hydroxyl ion (OH⁻) attachment sites for nucleation with density exceeding 10¹² cm⁻². The nebulized aqueous precursor impinges on a substrate heated to ~300 °C, giving growth rate exceeding 200 nm/min. Substrate heating provides reaction activation energy, decomposing and volatilizing reaction byproducts at temperatures well below those required for pyrolysis. Fig. 1 (left) presents a photograph of the apparatus used to grow our BaTiO₃ films, which were subsequently annealed in the range 500 – 600 C for 1 - 2 hours.

Physical characterization by scanning electron microscopy (SEM, Zeiss ULTRA-55 FEG) and asymmetric out-of-plane X-ray diffraction (XRD, PANalytical Empyrean #2) were performed at the UCF Materials Characterization Facility (MCF). The Cu K α X-ray beam at 0.1540598 nm was incident at a fixed angle of 1 deg.

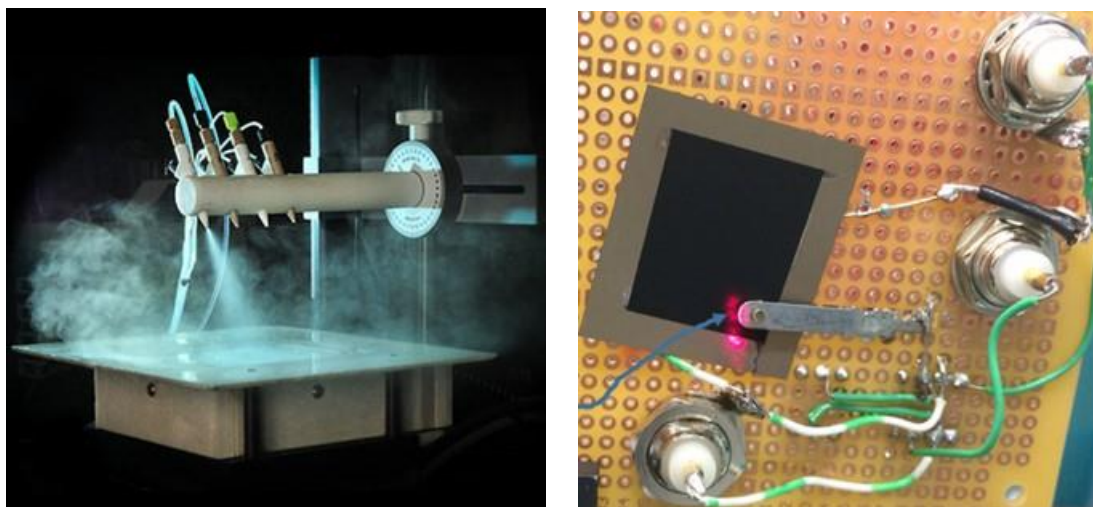


Figure 1. (left) Photograph of SPEED deposition system. (right) Photograph of experimental set up for photoresponse measurements. A spring contact connects to the carbon-black coating on the BaTiO₃ thin-film. The amplifier is constructed on the back side of the printed-circuit board. The arrow points to the spot of a red alignment laser which indicates the position illuminated by the pulsed CO₂ laser.

In preparation for photo-response measurements, a 4- μm -thick BaTiO₃ film on 75- μm -thick stainless steel foil substrate, which had been annealed 2 hours at 500 C, was coated with a conducting carbon-black IR absorbing layer. A gold-coated spring contact was made to the carbon black layer and connected to the inverting input of a type 741 operational amplifier, as shown in Fig. 2 (right). The substrate and non-inverting input of the op-amp were grounded. A 1 M Ω feed-back resistor was connected between inverting input and op-amp output, which was connected to a digital oscilloscope. Photoresponse was excited using a pulsed CO₂ laser (MTL-3 Mini TEA, Edinburgh Instruments) at 10 micron wavelength. Pulse duration was approximately 100 ns and repetition rate was 2 Hz. The peak power was not precisely measured, but the power in a single pulse was sufficient to cause a noticeable change in the color of liquid-crystal thermal paper designed for 25-30 deg operation (Edmund Optics R25C5W). The color change was similar to that caused by a 100 mW CW CO₂ laser, allowing an estimate of 50 mJ per pulse. This value is the same order as that specified in the laser manual.

Results

Fig. 2 (left) presents a top-view SEM image. The film comprises a sea of nano crystals, in which are embedded micron-sized single-crystal islands. Fig. 2 (right) presents a cross sectional SEM image of the film, revealing a 2 μm film thickness.

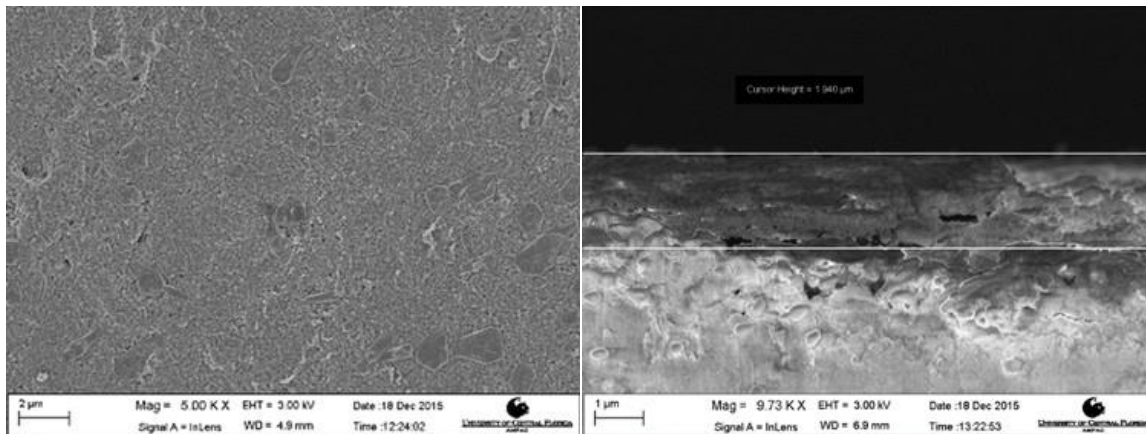


Figure 2. SEM images of SPEED-grown BaTiO₃ films. (left) top view revealing mix of nano- and micro-meter scale crystals. (right) SEM cross section.

Fig. 3 presents XRD spectra for two different annealing temperatures indicated. Reference spectra are also presented, showing that the sample annealed at 500 C is most probably hexagonal phase, while the sample annealed at 600 C has very clearly converted to the non-pyroelectric cubic phase. Notable differences are that the latter is missing the peaks evident in the spectrum of the former near 18, 37, 49, 59, 68, and 69 degrees.

Both measured spectra contain peaks that are absent from either reference spectrum. Extra peaks at 24, 34 and 42.5 deg are stronger in the 600-C-annealed sample, which also contains an extra line at 46 deg absent for the 500-C-annealed sample. These extra peaks suggest the presence of a different material that tends to increase on annealing at 600 C. However, analysis shows that this different material is not the rhombohedral, orthorhombic, or tetragonal BaTiO₃ phases, which tend to have fewer but similarly positioned peaks in their reference spectra compared with the hexagonal phase. Peaks

observed near 26, 37, 49, 59, 65, 68, and 69 degrees appear to be unique signatures of the hexagonal phase.

The intensity pattern for cubic phase is exactly like that in the powder XRD reference spectrum. Cubes have almost the same symmetry as spheres, so any preferred orientation should affect the XRD pattern less than for lower symmetry phases. The measured intensity pattern for the 500 C annealed sample agrees poorly with that for the hexagonal powder XRD reference. However, this low symmetry phase might well have a preferred orientation that would cause its intensity pattern to differ from that of the powder reference.

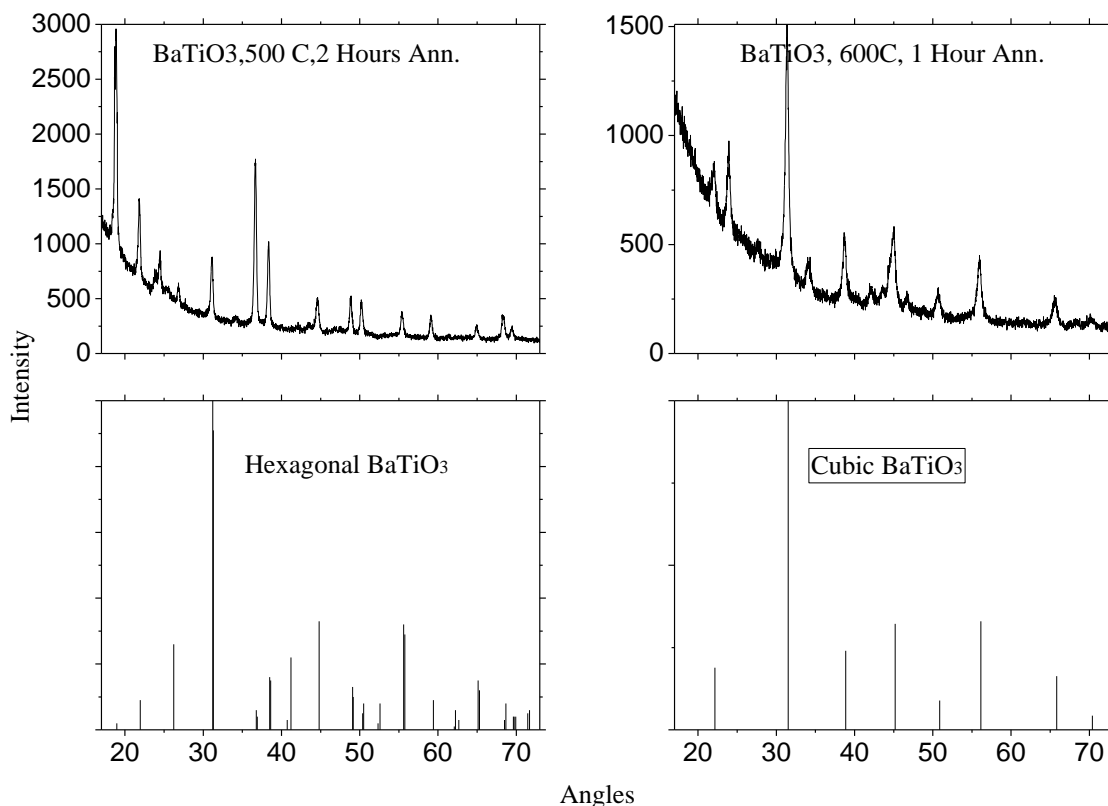


Fig. 3. XRD spectra of SPEED-grown BaTiO₃ thin films.

Fig. 4 (left) presents an AC-coupled oscilloscope screen shot with a response transient for a sample annealed at 500 C for 2 hours. The decay time is about 5 ms. There is strong electrical disturbance due to the laser pulsing circuit at times earlier than shown, with the result that when the laser beam is shuttered, there is a negative signal of about the same magnitude in the region indicated by the boxcar gate (channel 2). Thus, the peak photo response is about 400 mV, or 8 V/J for the sample and amplifier combination. This signal was 10x stronger than for a similar sample annealed half as long (1 hr at 500 C).

Fig. 4 (right) presents a measurement of photo-response as a function of position on the 1 cm² area of the carbon-black coating. The sample was translated using an x-y stage. The point (0,0) corresponds to the center of the sample. The x-scan was performed at y = 0 and vice versa. The photo response appears to be fairly uniform across the active area, dropping steeply the edges of the carbon-black square.

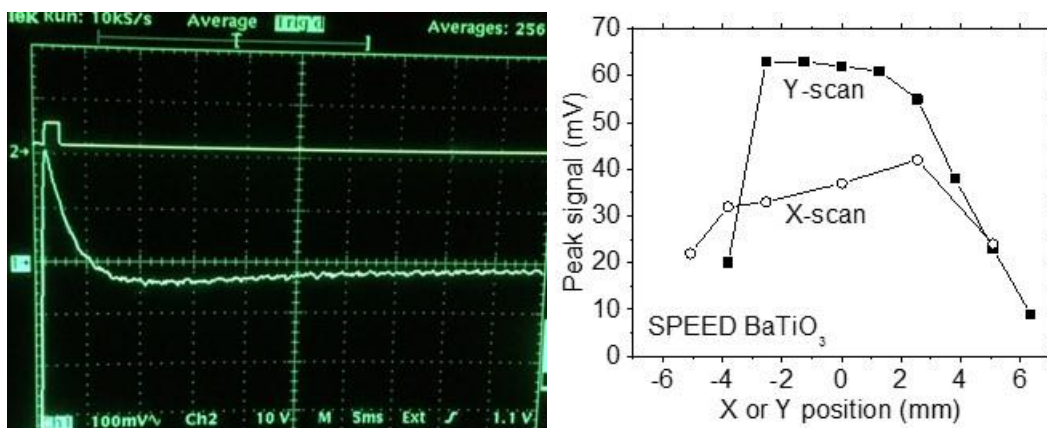


Fig. 4. (left) Oscilloscope screen shot showing the transient pyroelectric response to the laser pulse on channel 1. Channel 2 shows the gate of a boxcar averager. (right) Peak signal as function of position on the absorbing area of the BaTiO₃ device.

Note that the signal strength in Fig. 4 (right) is smaller than in Fig. 4 (left), which was measured about one week earlier. The photo-response was found to decay over time, presumably due to the absorption of water vapor from the air. Fig. 5 (left) presents a plot of 4 measurement points collected over a period of 3 weeks, showing a characteristic decay time of 1 week. Baking at 100 C restores the response, as shown in Fig. 5 (right).

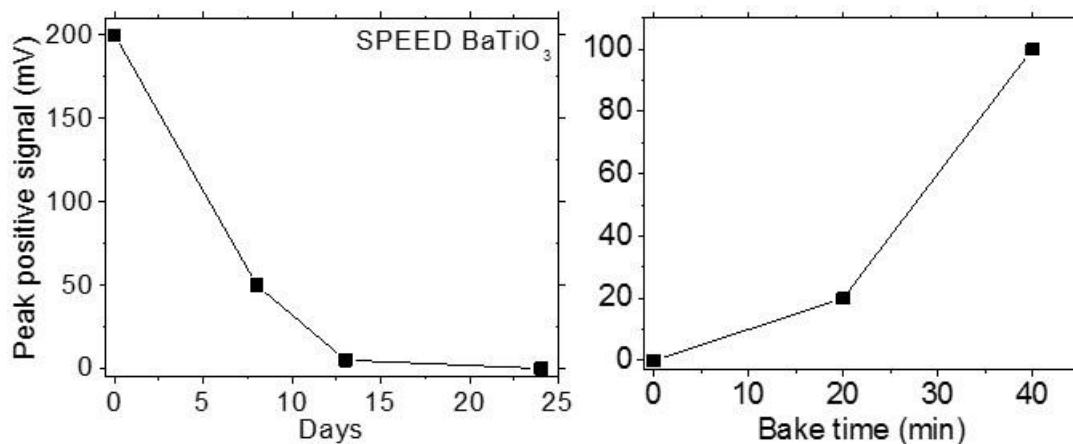


Fig. 5. (left) Decay in peak photo-response with time for sample kept in air. (right) Recovery of signal on baking at 100 C.

Poling experiments were performed on the sample on day 13 (Fig. 5), when the signal had decayed almost to zero. This was achieved by applying a DC voltage between top and substrate surfaces of the sample with the op-amp power turned off. Voltages of 0.5 and 1 V applied for 2 minutes produced no effect. Voltages of 2 V applied for 2 minutes produced a negative signal with -40 mV peak amplitude, and this signal had the opposite sign from the original signal of the unpoled sample. The signal achieved by poling decayed in ~1 min. The sample could be poled again, and the behavior was repeatable. When poling of the opposite sign was applied, the photoresponse was positive.

Conclusions

BaTiO₃ thin films were grown by an aqueous spray deposition process at moderate substrate temperatures. Two phases were observed depending on annealing temperature. The hexagonal phase demonstrated a pyroelectric infrared photoresponse.

Acknowledgment

This work by Mr. Alhasan was supported in part by the Higher Committee for Education Development in Iraq (HCED), Prime Minister Office, Baghdad, Iraq, <http://hcediraq.org/>.

References

1. M. M. Vijatović, J. D. Bobić and B. D. Stojanović, *Science of Sintering*, **40**, p. 235 (2008).
2. Genc Hyseni, Nebi Caka and Kujtim Hyseni, *Advanced Research in Physics and Engineering*, p. 161 (2010).
3. Sea-Fue Wang, Yung-Fu Hsu, Yu-Wen Hung and Yi-Xin Liu, *Appl. Sci.*, **5**, p. 1221 (2015).
4. Pingsheng Tang, D. J. Towner, T. Hamano, and A. L. Meier, *Optics Express*, **12**, p. 5962 (2004).
5. F. A. Yildirim, C. Ucurum, R. R. Schlieve, W. Bauhofer, R. M. Meixner, H. Goebel, W. Krautschneider, *Appl. Phys. Lett.*, **90**, p. 083501 (2007).
6. Daniel Hernandez Cruz, and Roger A. Lessard, *Proc. SPIE*, **4804**, p. 9 (2002).
7. L. D. Landau, E. M. Lifshitz, and L. P. Pitaevskii, *Electrodynamics of Continuous Media*, section 13, Elsevier, Butterworth, Heinemann, Amsterdam (1984).
8. L. Simon-Seveyrat, A. Hajjaji, Y. Emziane, B. Guiffard and D. Guyomar, *Ceramics International*, **33**, p. 35 (2007).
9. F. Amy, A. Wan, A. Kahn, F. J. Walker and R. A. McKee, *J. Appl. Phys.*, **96**, p. 1601 (2004).
10. Chang-Tai Xia, Er-Wei Shi, Wei-Zhuo Zhong and Jing-Kun Guo, *J. European Ceramic Society*, **15**, p. 1171 (1995).
11. Margarita García-Hernández, Antonieta García-Murillo, Felipe de J. Carrillo-Romo, David Jaramillo-Vigueras, Geneviève Chadeyron, Elder De la Rosa and Damien Boyer, *Int. J. Mol. Sci.*, **10**, p. 4088 (2009).
12. Kyo Kwang Leea, Yun Chan Kangb, Kyeong Youl Junga and Jung Hyun Kimc, *J. Alloys and Compounds*, **395**, p. 280 (2005).
13. Adelina Ianculescu1, Sophie Guillemet-Fritsch and Bernard Durand, *Processing and Application of Ceramics*, **3**, p. 65 (2009).
14. Jesús Prado-Gonjal, Rainer Schmidt and Emilio Morán, *Microwave-assisted Synthesis and Characterization of Perovskite Oxides*, Novascience Publishers, **4**, p. 117 (2013).
15. Yasuhisa Yamashita, Hiroshi Yamamoto and Yukio Sakabe, *Japanese J. Applied Physics*, **43**, p. 6521 (2004).
16. E. J. H. Lee, F. M. Pontes, E. R. Leite, E. Longo, J. A. Varela, E. B. Araujo and J. A. Eiras, *J. Materials Science Letters*, **19**, p. 1457 (2000).

17. Ying Yuan, Shuren Zhang and Wennan You, *Materials Letters*, **58**, p. 1959 (2004).
18. C.N. Georgea, J.K. Thomasb, , H.P. Kumarb, M.K. Sureshb, V.R. Kumarc, P.R.S. Wariarc, R. Jose and J. Koshya, *Materials Characterization*, **60**, p. 322 (2009).